COVID-associated pulmonary aspergillosis in immunocompetent patients

Henrique AL Ribeiro[1], Yogesh Scindia[1], Borna Mehrad[1†] and Reinhard Laubenbacher[1*†]

[1]Department of Medicine, Division of Pulmonary, Critical Care, and Sleep Medicine, University of Florida, Gainesville, 32610, FL, U.S.A.

*Corresponding author(s). E-mail(s): reinhard.laubenbacher@medicine.ufl.edu;
Contributing authors: henrique.deassis@medicine.ufl.edu; yogesh.scindia@medicine.ufl.edu; borna.mehrad@medicine.ufl.edu;
†Co-last-authors

Abstract

Purpose: The opportunistic fungus *Aspergillus fumigatus* infects the lungs of immunocompromised hosts, including patients undergoing chemotherapy or organ transplantation. More recently however, immunocompetent patients with severe SARS-CoV2 have been reported to be affected by COVID-19 Associated Pulmonary Aspergillosis (CAPA), in the absence of the conventional risk factors for invasive aspergillosis. This paper explores the hypothesis that contributing causes are the destruction of the lung epithelium permitting colonization by opportunistic pathogens. At the same time, the exhaustion of the immune system, characterized by cytokine storms, apoptosis, and depletion of leukocytes may hinder the response to *Aspergillus* infection. The combination of these factors may explain the onset of invasive aspergillosis in immunocompetent patients. **Methods:** We used a previously published computational model of the innate immune response to infection with *Aspergillus fumigatus*. Variation of model parameters was used to create a virtual patient population. A simulation study of this virtual patient population to test potential causes for co-infection in immunocompetent patients.

Results: The two most important factors determining the likelihood of CAPA were the inherent virulence of the fungus and the effectiveness of the neutrophil population, as measured by granule half-life and ability to kill fungal cells. Varying these parameters across the virtual patient population generated a realistic distribution of CAPA phenotypes observed in the literature. **Conclusions:** Computational models are an effective tool for hypothesis generation. Varying model parameters can be used to create a virtual patient population for identifying candidate mechanisms for phenomena observed in actual patient populations.

Keywords: COVID-19, invasive aspergillosis, coinfection, immunocompetent host, computational model, virtual patient population

1 Introduction

Aspergillus fumigatus is an opportunistic fungus that can infect the lungs of immunocompromised hosts, including, among others, patients undergoing chemotherapy or receiving an organ transplant, and patients affected by chronic granulomatous disease [1, 2]. Neutrophils are essential to fighting the pathogen, and impaired neutrophil responses are a common predisposing factor to the infection. More recently, patients with severe SARS-CoV2 infection have reportedly been affected by COVID-19 Associated Pulmonary aspergillosis (CAPA). However, Lai, CC, and Yu, W 2021 [3] found that the conventional risk factors for aspergillosis were not present in CAPA patients.

Mitaka, H *et al.* 2021 [4] found that around 10% of COVID-19 patients in ICUs develop invasive aspergillosis, and the mortality rate for these patients is 54% compared with 24% of those without CAPA [5]. According to Lai, CC, and Yu, W 2021 [3], patients with CAPA are predominantly male, with an average age of 73±13 years, and 88% had diabetes, high blood pressure, kidney disease, chronic obstructive pulmonary disease (COPD), or heart disease. The fact that CAPA is associated with these comorbidities but not with the conventional risk factors for invasive aspergillosis requires the generation of new hypotheses to explain the susceptibility of these hosts to the infection.

Computational models have been used extensively in immunology to create and test hypotheses. In particular, agent-based models have proven effective for studying respiratory diseases. They are intuitive, rule-based models that make it easy to represent heterogeneous spatial environments and individual entities, such as immune cells or pathogens, and their generation does not require extensive modeling expertise. We published an agent-based model of the innate immune response to *Aspergillus fumigatus* within an alveolar duct that established that one of the critical parameters determining infection outcome is the distance within which macrophages can detect fungal spores [6].

In [7], we published an agent-based model of the immune response to *Aspergillus fumigatus*. The model focuses on the role of iron sequestration by

the host as part of the innate immune response. It was parametrized entirely with information from the literature rather than data fitting, and was extensively validated with both data from the literature and our own time course data from experiments using a mouse model of the infection. We also showed that variation of parametrizations from this reference model could account for the variability across experiments. A first result we obtained using the model demonstrates that fungal strains engage different parts of the innate immune response depending on their level of virulence. This computational model is the main tool for the results reported here.

We hypothesize that in patients with severe COVID-19, the destruction of the lung epithelium facilitates colonization by opportunistic pathogens. At the same time, the exhaustion of the immune system characterized by cytokine storms, apoptosis, and depletion of leukocytes hinders its ability to kill the fungus, explaining the susceptibility of otherwise immunocompetent patients to aspergillosis. We use the computational model to test this hypothesis and to ask what set of parameters and conditions explain CAPA. To test our hypothesis, we created a virtual patient population by sampling the model parameter space, characterizing patients with dual infection and analyzing disease outcomes, with each choice of parameters representing one virtual patient.

2 Modeling

The current work uses a previously published model [7] that simulates the innate immune response to *Aspergillus fumigatus* in immunocompetent hosts. The model spans the intracellular, tissue-level, and organism scales. At the tissue level, an agent-based model simulates the immune response in a spatially homogeneous representation of a volume of lung tissue. Its components are depicted in Figure 1. The model contains 76 parameters, all obtained from the literature rather than data fitting. This ensures a broader validity of the model beyond the data used to calibrate it.

For this study, we introduce minor modifications to the model in order to simulate an infection with *A. fumigatus* in a host with simultaneous viral pneumonia. We model this coinfection implicitly by changing certain parameters as well as the number of leukocytes in the lung space. In the model, neutrophils kill hyphae by direct contact. However, to accommodate alternative mechanisms of neutrophil anti-microbial function, we introduced a second scenario in which leukocytes secrete granules that diffuse and kill the fungus. The results for the second scenario are presented in the supplementary material. For the second scenario, we introduced the parameters (Kd_Granule and Granule_HALF_LIFE - Table A1). Upon interaction with *Aspergillus*, neutrophils are activated and then secret one arbitrary unit of granule (an abstraction for the molecules contained in neutrophil granules). This granule kills hyphae with a probability given by Equation 1. The granule contents, like all molecules,

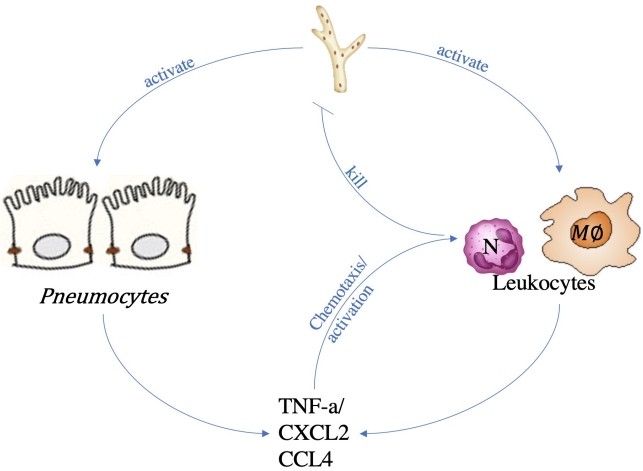

A

Fig. 1 Model description. *Aspergillus fumigatus* hyphae activate host cells (pneumocytes, monocytes, and neutrophils). These cells, chiefly pneumocytes and monocytes, secrete cytokines (TNF-α and IL-10) and chemokines (CXCL2 and CCL4). The chemokines chemoattract leukocytes (neutrophils and monocytes) to the infection sites, and the cytokines (TNF-α), together with the fungus itself, activate the leukocytes. Leukocytes kill *Aspergillus*. This simplified figure does not show inactivation by IL-10/TGF-β/apoptotic cells and the secretion of TGF-β by inactivated cells.

decay with a half-life (Granule_HALF_LIFE):

$$p = 1 - e^{-x/k_d}, \tag{1}$$

where x is the granule concentration in arbitrary units and k_d is k_d_Granule. We choose values for k_d_Granule and Granule_HALF_LIFE to fit data in [7].

In [7], iron sequestration acted to inhibit *Aspergillus* growth. Here we do not consider the role of iron explicitly. Instead, we tested a wide range of hyphal growth rates (Table 1) to represent more or less permissive lung environments, partly as the result of variable availability of nutrients such as iron across the space (see below). Another contributing factor is the damage done to the epithelium by the ongoing viral infection.

In this study, we focus on five parameters, with values listed in Table 1. The first parameter is the intrinsic growth rate of the fungus. The second and third parameters are proxies for the strength of the immune response, and the fourth and fifth parameters reflect an increased number of immune cells as part of the response to the viral infection. The intrinsic growth rate of the hyphae encapsulates the permissivity of the environment, such as the nutrient availability. However, the collective effects of the intrinsic growth rate, together with the counteracting effects of the immune response, we call observed growth rate.

Table 1 Model parameter ranges. The table shows the ranges in which we sample parameters (maximum and minimum value). Column 1: parameter name; Column 2: description; Column 3: parameter range; Column 4: parameter reference value; Column 5: rationale for the value in Column 4. The values taken from [7] are the default values in our previous work.

Parameter	Description	Parameter range	Reference Value	Ref
GROWTH_RATE	intrinsic growth rate	2.75-80 $\mu m/h$	40 $\mu m/h$	[7]
PR_N_KILL	probability of neutrophils to kill hyphae	0.23-23%	23%	[7]
PR_MA_KILL	probability of monocytes to kill hyphae	0.099-9.9%	9.9%	[7]
MAX_M	number of monocytes	360-960 cells	960 cells	[8]
MAX_N	number of neutrophils	360-960 cells	360	[8]

With these minor changes, we proceeded with our simulation study. We used a regular grid of 10X10X10 voxels, each with 40X40X40 μm ($6.4 \times 10^{-2} \mu L$). We initialize the grid with 640 type-II pneumocytes (see [7]), while monocytes and neutrophils vary between 360-960 (Table 1). The leukocyte number was kept constant throughout the simulation, unlike in our previous work. The rationale for these values is derived from [8], which shows that after two or three days with influenza, mice have approximately 5 million neutrophils and 15 million monocytes. Because we are simulating a volume of $6.4 \times 10^{-2} \mu L$ and a pair of mouse lungs has a volume of 1 mL [9], these numbers (5-15 million) translate into 360-960. It is essential to note that according to the work of Gong, D. *et al.* 2011 [8], we should set monocytes to 960 and neutrophils to 360; however, because we want to test the importance of changing these cell numbers, we vary both in the range 360-960. Each simulation was comprised of 720 iterations or 24 hours of simulation, with a time-step of 2 minutes. We used periodic boundary conditions. In addition to the cells listed above, we also included the cytokines and chemokines TNF-α, IL-10, TGF-β, CXCL2, and CCL4. The chemokines help guide cells to the infection loci but did not increase the number of leukocytes in the simulated volume. TNF-α activates monocytes while IL-10 and TGF-β inactivate them. Like in our previous model, only activated monocytes are able to kill hyphae, while neutrophils in any state of activation are able to kill the fungus.

We performed Latin-Hypercube Sampling (LHS) on the parameters in Table 1. We varied the number of leukocytes, the monocyte killing probability (the probability with which monocytes kill hyphae upon direct contact), the intrinsic growth rate, and the neutrophil killing probability (the probability with which neutrophils kill hyphae upon direct contact). Note that, in general, the maximum value for each parameter is the default in [7] (see Table 1). The intrinsic growth rate of 40 $\mu m/h$ is the default in our previous work, albeit [10] shows that this value can be as high as 60 $\mu m/h$. However, due to the iron acquisition bottleneck, the initial apparent growth rate (i.e., the observed growth rate in the absence of an immune response) in our previous model was $3\mu m/h$. Therefore, here we are testing what happens if the fungus grows unencumbered.

Using LHS sampling we generated 24,000 parameter sets, representing 24,000 virtual hosts of the dual infection. (We also createad an aditional 36,000 virtual hosts using the alternative neutrophil mechanism; see supplementary

material). We measured the observed growth rate as the slope of the log of the *Aspergillus* curve (Equation 2). Note that we shifted the *Aspergillus* curve by 1 to avoid negative infinity when the number of *Aspergillus* cells tends to zero. The observed growth rate is an empirical value given by Equation 2, while the intrinsic growth rate is a model parameter (Table 1). Like in our previous work, we define each hyphal septae as a "hyphae-cell."

$$Log_{10}(hyphae + 1) = a + b \times t, \tag{2}$$

where b is the observed growth rate, and t is time in hours.

It is important to observe that hyphae are capable of linear extension (elongation) and branching. Both contribute to the growth of hyphal colonies. However, the intrinsic growth rate is equal to the elongation rate. The branching probability is 25% for every 30 minutes [7].

Partial Rank Correlation Coefficient

To compute partial rank correlation by growth rate, we divided the 24,000 data points into ten bins of similar intrinsic growth rates (GROWTH_RATE). Then we computed the partial rank correlation coefficient of the other four parameters (PR_N_KILL, PR_MA_KILL, MAX_MA, and MAX_N) against the observed growth rate using the method "pcc" from the R package "verification" [11]. Finally, we squared the partial correlations and performed 100 bootstraps.

3 Results

Our goal is to test the hypothesis that a respiratory viral infection such as severe COVID-19 can make the lung environment more permissive to *Aspergillus* growth and, at the same time, exhaust the immune system, allowing the fungal infection to progress in an otherwise immunocompetent host. In the simulator, these conditions translate into a higher intrinsic growth rate and lower ability of leukocytes to kill hyphae. Concomitantly, when the *Aspergillus* infection starts, the number of leukocytes in the lung is high because the host is already fighting another infection. These conditions are encoded by the model parameters in Table 1. Each parameter sample can be thought of as a virtual patient for whom we simulate infection outcome. We started each simulation with 640 type-II pneumocytes, 20 germinated conidia, and 360-960 monocytes and neutrophils and ran it for 720 iterations (24 simulated hours). The results are shown in Figure 2.

In order to correctly interpret Figure 2, one needs to keep in mind the distinction between intrinsic growth rate and observed growth rate. The first is a parameter (Table 1) that controls the time it takes for new *Aspergillus* cells to be generated. The second results from the number of cells generated (intrinsic growth rate) minus the number of cells killed by leukocytes. The intrinsic growth rate is always positive, while the observed growth rate may be negative if the infection is declining, as observed in the vast majority of cases in Figure 2.

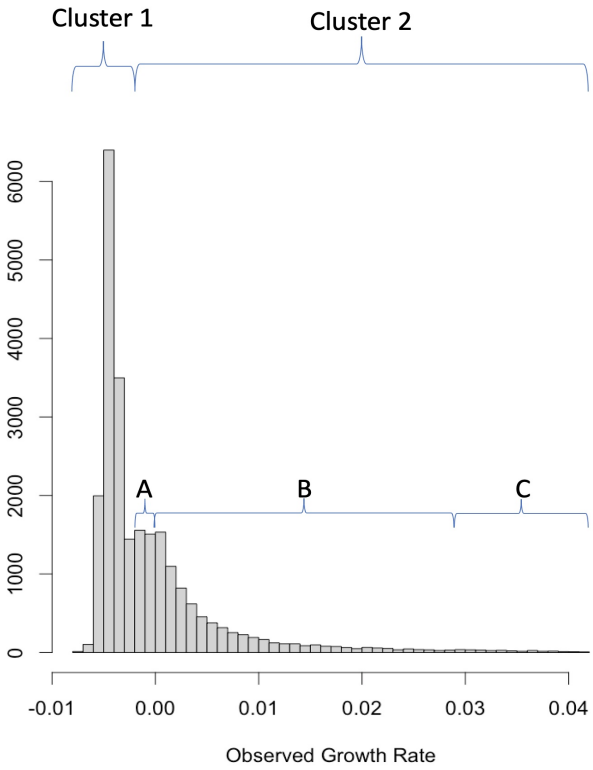

A

Fig. 2 Distribution of observed growth rate. We divided virtual patients into two clusters: the prominent peak on the negative side (Cluster 1) and the secondary peak (Cluster 2). We then subdivided Cluster 2 into three subclusters: 2A is the negative part, 2B is the positive part excluding outliers, and 2C is the long tail of outliers.

The data in Figure 2 show a prominent peak in negative observed growth rate, indicating resolution of the infection, and a second smaller peak with a long tail of positive observed growth rate. We can therefore cluster patients into two groups, with Cluster 1 containing only patients that clear the infection. Cluster 2 can be further subdivided into three subclusters representing progressively worsening fungal infection. Cluster 2A is the portion of Cluster 2 with negative observed growth rate, representing patients whose infection clears, while Cluster 2B is the portion of Cluster 2 with positive observed growth rate (excluding the outliers), and Cluster 2C is the long tail of outliers (Figure 2), both together representing patients that develop CAPA. This binomial distribution is consistent with what is known for this disease: patients with an intact neutrophil response resolve the fungal infection, whereas the cluster with positive observed growth rate corresponds to the observation that COVID-19 patients in the ICU can develop CAPA [4].

Clusters 2B and 2C in Figure 2 suggest that a combination of higher intrinsic fungal growth rate and lower fungal killing by the immune response can explain the onset of CAPA in otherwise immunocompetent hosts. To further explore this hypothesis, we constructed classification trees to see which combinations of parameters are necessary for CAPA (Figure 3).

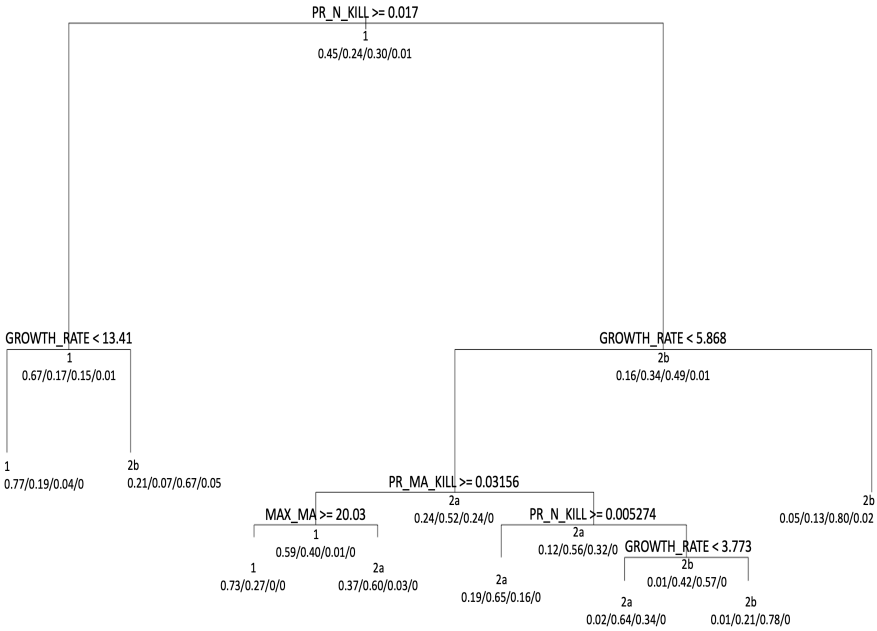

A

Fig. 3 Classification tree. The classification tree found the parameter values that best parse the virtual patients into the four clusters defined in Figure 2. Percentage value range is 0-1.

One can see in Figure 3 that the dominant parameters are the neutrophil killing rate, intrinsic growth rate, and to a lesser degree, the monocyte killing rate. Classification trees can indicate which parameters are the most important by measuring how much each parameter contributes to node purity. We confirmed that these three parameters (neutrophil killing rate, intrinsic growth rate, and monocyte killing rate) are indeed the dominant ones.

Since we have only three dominant parameters, we can plot the virtual patients in a 3D space. That will allow us to see how the four clusters are distributed. In Figure 4A, each point represents a virtual patient. The x-axis is the log of that patient's intrinsic growth rate, the y-axis is the log of that patient's monocyte killing probability, and the z-axis is the log of that patient's neutrophil killing probability. We colored each patient according to their cluster (1, 2A, 2B, or 2C). We used log base ten because different patients have parameter value differences of up to two orders of magnitude.

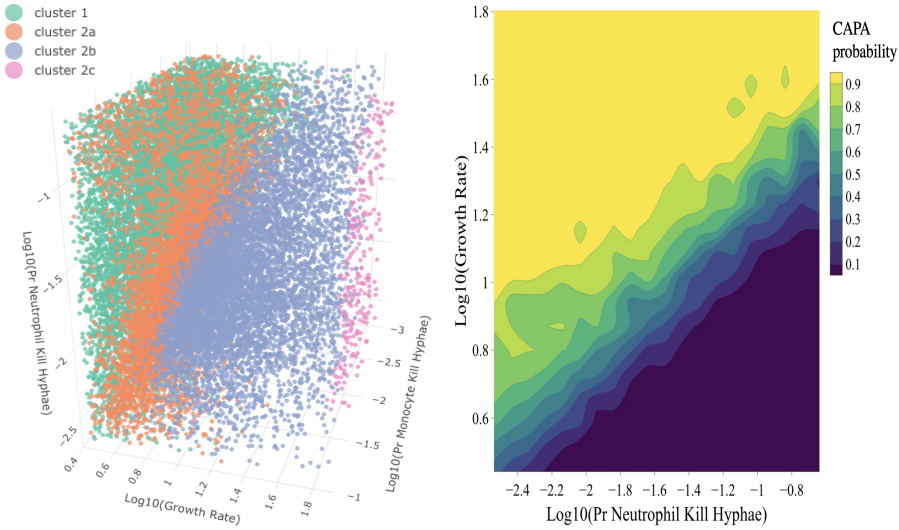

A B

Fig. 4 Plots in 3D space of the most important parameters according to the classification tree (Figure 3). Figure 4A virtual patients plotted in 3D space. The x-axis is the log of patients' intrinsic growth rate, the y-axis is the log of their monocyte killing probability, and the z-axis is the log of the neutrophil killing probability. Figure 4B shows the CAPA probability as the intrinsic growth rate and neutrophil killing probability change.

As shown in Figure 4A, Clusters 1 and 2A are interspersed. This is to be expected because both these clusters represent patients for whom the infection cleared (Cluster 2A is the negative part of peak 2). Cluster 2C is segregated in the high intrinsic growth rate region. However, it is noteworthy that some patients in Cluster 2B are very similar to patients in Cluster 2A, in that they have similar sets of parameters that characterize their infection.

To better explore this transition between patients that clear the infection (Clusters 1 and 2A) and those that do not (Clusters 2B and 2C), we computed how the probability of developing CAPA changes as parameters vary (Figure 4B). We restrict ourselves to plotting the CAPA probability across the two most influential parameters. We plot how a virtual patient's probability of developing CAPA changes as the intrinsic growth rate and the neutrophil killing rate change (Figure 4B). As shown in Figure 4B, the cliff where a patient may either clear the infection or develop CAPA cuts the graph across the diagonal. Both parameters (intrinsic growth rate and neutrophil killing probability) are essential in determining the patient's outcome: a high intrinsic growth rate can be compensated for, in part, by a high killing rate and vice versa.

An essential question in Figure 4, especially 4B, is whether using only two parameters is meaningful. To answer that question, we divided the virtual patients into two subsets. The first subset of 20,000 was used to train classification trees, while the second subset of 4,000 was used to test its predictive

Table 2 The predictive power of parameters. The predictive power of classification trees was evaluated in cross-validation and test sets when these trees were trained using all five parameters, the top three parameters (GROW_RATE, PR_N_KILL, and PR_MA_KILL), or the top two (GROW_RATE and PR_N_KILL). Column 1 parameters used in the model; Column two F1 score in cross-validation; Column 3 F1 score in the test set.

Parameters	F1-cross-valildation	F1-test
ALL	0.7379	0.7430
Top-three	0.7380	0.7393
Top-two	0.7108	0.7163

power. We also used ten-fold cross-validation and measured the F1 score, as in Table 2. The F1 score combines the precision and recall into a single metric, and it is primarily used to compare the performance of a classifier. We found that the reduction from all five parameters to the top three (GROW_RATE, PR_N_KILL, and PR_MA_KILL) does not affect the predictive power of the classification trees, while the reduction to the top two (GROW_RATE and PR_N_KILL) has only a minor effect.

As Figure 3 suggests, the parameters exhibit synergy with each other. For instance, depending on the value of the intrinsic growth rate, the neutrophil killing rate may be more or less influential. In Figure 5, we plot the correlation of the parameters with the observed growth rate as the intrinsic growth rate changes. Figure 5 shows the square of the partial ranking correlation between neutrophil killing rate and observed growth rate. The correlation between these two variables is negative (results not shown) for neutrophils kill hyphae. Interestingly, this correlation is more substantial for intermediate values of the intrinsic growth rate. The partial correlation between the other parameters and the observed growth rate was not substantial (results not shown).

4 Discussion

Aspergillus fumigatus is an opportunistic mold that infects immunocompromised hosts, chiefly those with impaired neutrophil response, but also patients with normal neutrophils but impaired cell-mediated immunity [12]. However, Lay, C, and Yu, W 2021 [3] found that in patients with CAPA the conventional risk factors for invasive aspergillosis are not present. They found that CAPA patients were mostly older men suffering from diabetes, obesity, hypertension, or cardiovascular disease. These conditions may help explain the onset of CAPA, but are likely not sufficient by themselves. We hypothesized that COVID-19 infection may exhaust the immune system, and at the same time the destruction of lung epithelium overloads the fungus with nutrients. We tested this hypothesis using a simulated virtual patient population generated by our computational model in [7].

Our simulations showed that only 31% of the virtual patients with COVID-19 who were exposed to *Aspergillus* developed CAPA (Figure 2). That is qualitatively consistent with observations that only 10% of COVID-19 patients in ICU develop invasive aspergillosis [4]. The discrepancy in the exact value can

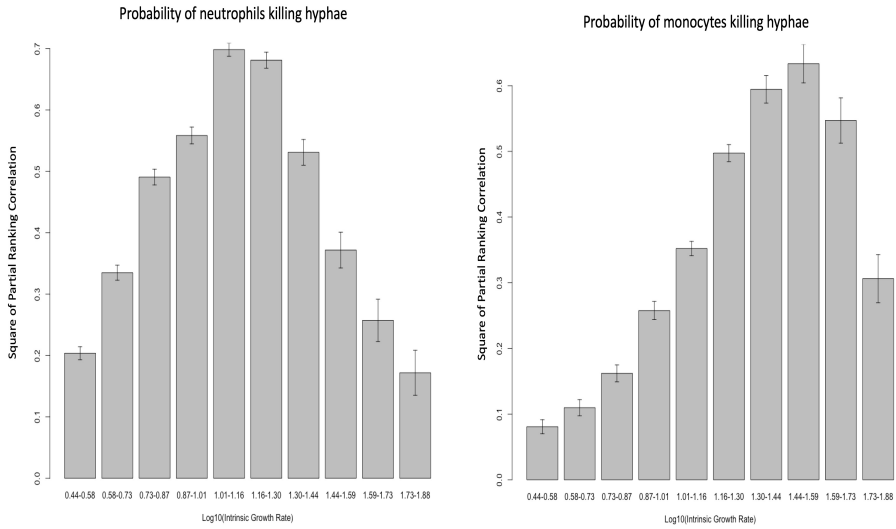

A B

Fig. 5 Variation of the square of the correlation r^2 between the critical model parameters and the observed growth rate, with the variation of the intrinsic growth rate. We started with a dataset of 24,000 virtual patients generated with LHS and then partitioned this dataset by intrinsic growth rate. The x-axis shows the range of the intrinsic growth rate in each partition. We then calculate the correlation between parameters and the observed growth rate in each partition. Figure 5A: Variation of r^2 between the neutrophil killing rate and observed growth rate. Figure 5B: Variation of r^2 between monocyte killing rate and observed growth rate. Error bars are standard deviations calculated with bootstrap.

be explained by the fact that most patients hospitalised with COVID-19 infection are presumably not exposed to *Aspergillus*. In addition, virtual patients are a random sample of the parameter space, while actual patients may have a bias toward CAPA resistance. However, one must notice that in the alternative scenario where neutrophils do not need direct contact to kill *Aspergillus* (Supplementary material), only 17% of VPs developed invasive aspergillosis (Figure A1).

Our model suggests that both reducing neutrophil activity and increasing fungal intrinsic growth rate might be necessary for CAPA to emerge (Figures 3 and 4). Grunwell, JR *et al.* 2018 [13] found that neutrophils treated with airway supernatant of patients with acute respiratory failure due to lower respiratory tract viral infection had altered surface markers. Moreover, when the neutrophils were treated with airway supernatant in patients with bacterial and viral coinfection, they had decreased respiratory burst and bactericidal response. The mechanism is not well understood. However, Verweij, PE *et al.* 2020 [14] reported that influenza might suppress neutrophil oxidative burst, causing temporary disease status resembling chronic granulomatous disease. Arastehfar, A *et al.* 2020 [15] indicate that collateral effects of antiviral immunity may, paradoxically, contribute to an inflammatory environment that favors secondary infections such as CAPA. On the other hand, the drugs used to

treat serious COVID-19 infection, such as Tocilizumab and dexamethasone, can also hinder the immune response against *Aspergillus* [16]. These findings support the hypothesis that the immune response against *A. fumigatus* may be hampered in patients with serious COVID-19 infection.

Concomitantly, Escobar, N *et al.* 2016 [17] showed that pneumocytes cocultured with *A. fumigatus* inhibited fungal germination and growth. In contrast, Rodrigues, AG *et al.* 2005 [18] found that exposing *Aspergillus* to albumin increases its germination and growth rate. Furthermore, iron concentration, a bottleneck in our previous model [7], may be higher in serum than in the alveolar space [19]. Arastehfar, A *et al.* 2020 [15] argue that the leading risk factor for CAPA includes severe lung damage during the course of COVID-19 and the presence of comorbidities such as structural lung defects. These findings support our hypothesis that lung epithelium destruction favors *Aspergillus* growth: once the pneumocytes are killed, *Aspergillus* is exposed to a nutrient-rich environment and can grow faster.

Figure 4 shows that the onset of CAPA is regulated chiefly by the intrinsic fungal growth and neutrophil killing rates. The CAPA probability increases as the intrinsic growth rate increases or as the neutrophil killing probability decreases. In the alternative neutrophil action scenario (Figure A2), we can make a similar observation with granule K_d and intrinsic growth rate (Figure A2B). A moderate increase in the intrinsic growth rate and decrease in neutrophil activity can also lead to CAPA. Alternatively, a high increase in intrinsic growth rate or a steep decrease in neutrophil activity could also lead to the same outcome. Both scenarios we tested (i.e., neutrophils killing by direct contact or by secreting granules) support this conclusion. We found the first hypothesis to be more plausible (i.e., moderate change). However, Grunwell, JR *et al.* 2018 [13] found a substantial reduction in neutrophil killing ability that could support the second hypothesis (i.e., high change in neutrophil killing probability). However, whether their result generalizes to fungal coinfection remains open.

Figure 5 shows that neutrophils are more efficient in controlling the infection in the case of a moderate intrinsic growth rate. That corroborates the previous results. For low intrinsic growth rates, neutrophils can control the infection independent of their fungicidal properties (Figures 5A and 4B). Meanwhile, for high growth rates, even highly active neutrophils are ineffective against the disease. For monocytes, on the other hand, we found a bias toward a high growth rate that may reflect the fact that these leukocytes require a double interaction with *Aspergillus*, one to activate and one to kill. A high fungal concentration facilitates that. It is also interesting that the model was not sensitive to neutrophil and monocyte numbers (results not shown). We have a rough estimate of these cells from Gong, D. *et al.* 2011 [8]; however, the conclusions that we are deriving from this work are robust for a wide range of leukocyte concentrations.

We conclude that an increase in lung permissivity, probably due to an increased supply of nutrients and decreased effectivity of neutrophils to kill

hyphae, is the most likely explanation for CAPA. To make our findings more robust, we test two possible scenarios of how neutrophils kill hyphae. We found that the conclusions are the same, independent of the scenario.

- Funding: This work was partially supported by NIH grants DE021989, EB024501, AI135128, and AI117397; and NSF grant CBET-1750183
- Conflict of interest/Competing interests: The authors do not have any conflicts of interest or competing interests
- Ethics approval: The manuscript complies with the ethical standards of the Journal for Mathematical Biology.
- Consent to participate: Not applicable
- Consent for publication: All authors have approved the manuscript
- Availability of data and materials: Simulation data available on request
- Code availability: Code available upon request
- Authors' contributions: The study was conceived and carried out by HALR, with scientific input from the other authors. RL an BM provided funding for the project and contributed to the writing of the manuscript.

Appendix A Supplementary Material

Table A1 Model parameter ranges for the alternative scenario. The table shows the ranges in which we sample parameters (maximum and minimum value). Column 1: parameter name; Column 2: description; Column 3: parameter range; Column 4: parameter reference value; Column 5: rationale for the values in Column 4. The values taken from [7] are the default values in our previous work. The values for GROWTH_RATE, PR_MA_KILL, MAX_MA, and MAX_N are the same as in Table 1

Parameter	Description	Parameter range	Reference Value	Ref
GROWTH_RATE	intrinsic growth rate	2.75-80 $\mu m/h$	40 $\mu m/h$	[7]
PR_MA_KILL	probability of monocytes to kill hyphae	0.099-9.9%	9.9%	[7]
K_d-$Granule$	K_d of the reaction between granule and hyphae	1×10^{11} - 1×10^{13}	1×10^{13}	[7]
Granule_HALF_LIFE	granule half-life	0.033 - 3.33 h	0.67h	[7]
MAX_M	number of monocytes	360-960 cells	960 cells	[8]
MAX_N	number of neutrophils	360-960 cells	360	[8]

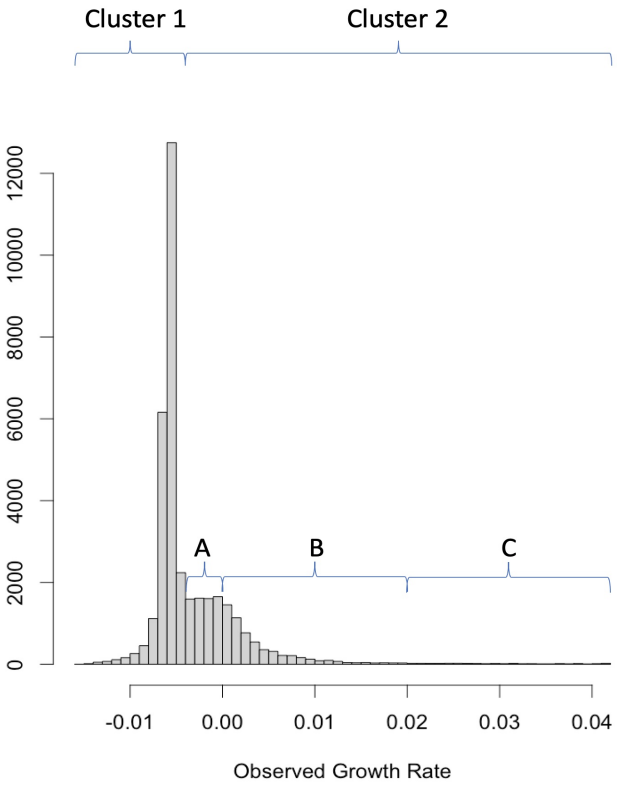

A

Fig. A1 Distribution of observed growth rate in the alternative scenario where neutrophils do not need direct contact to kill hyphae. We divided virtual patients into two clusters: the prominent peak on the negative side (Cluster 1) and the secondary peak (Cluster 2). We then subdivided Cluster 2 into three subclusters: 2A is the negative part, 2B is the positive part excluding outliers, and 2C is the long tail of outliers.

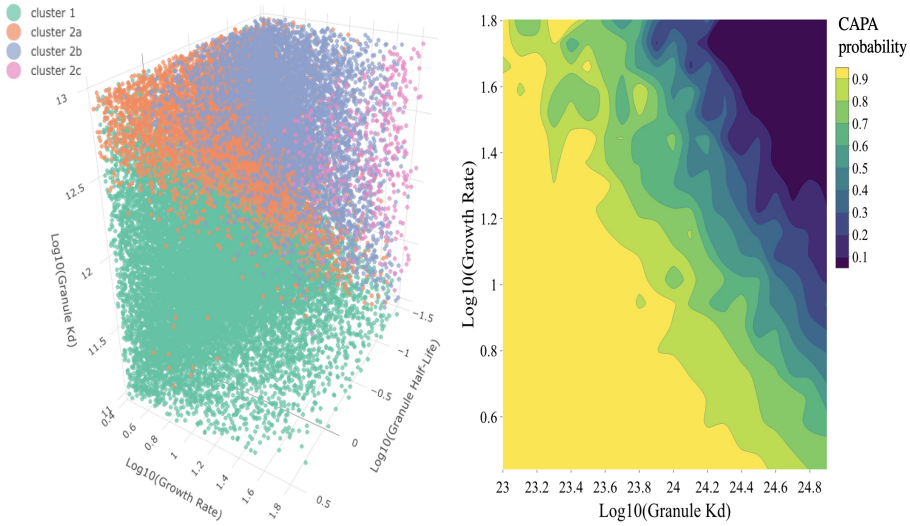

A B

Fig. A2 Plots in 3D space of the most important parameters according to the classification tree (not shown) in the alternative scenario where neutrophils do not need direct contact to kill hyphae. Figure A2A Virtual patients plotted in 3D space. The x-axis is the log of patients' intrinsic growth rate, the y-axis is the log of their neutrophils granule k_d, and the z-axis is the log of the neutrophil granule half-life. Figure A2B shows the CAPA probability as the intrinsic growth rate and neutrophil granule k_d change.

References

[1] Latge, J.-P.: Aspergillus fumigatus and aspergillosis. Clinical Microbiology Reviews **12**(2), 310–350 (1999) https://journals.asm.org/doi/pdf/10.1128/CMR.12.2.310. https://doi.org/10.1128/CMR.12.2.310

[2] Pappas, P., et al.: Invasive fungal infections among organ transplant recipients: results of the transplant-associated infection surveillance network (transnet). Clin Infect Dis **50**, 1101–11 (2010)

[3] Lai, C.-C., Yu, W.-L.: Covid-19 associated with pulmonary aspergillosis: A literature review. Journal of Microbiology, Immunology and Infection **54**(1), 46–53 (2021). https://doi.org/10.1016/j.jmii.2020.09.004

[4] Mitaka, H., Kuno, T., Takagi, H., Patrawalla, P.: Incidence and mortality of covid-19-associated pulmonary aspergillosis: A systematic review and meta-analysis. Mycoses **64**(9), 993–1001 (2021) https://onlinelibrary.wiley.com/doi/pdf/10.1111/myc.13292. https://doi.org/10.1111/myc.13292

[5] Ergun, M., Brüggemann, R.J.M., Alanio, A., Dellière, S., van Arkel, A., Bentvelsen, R.G., Rijpstra, T., van der Sar-van der Brugge, S., Lagrou, K., Janssen, N.A.F., Buil, J.B., van Dijk, K., Melchers, W.J.G., Reijers, M.H.E., Schouten, J.A., Wauters, J., Cordey, A., Soni, S., White, P.L., van de Veerdonk, F.L., Verweij, P.E., Hanson, K.E.: Aspergillus test profiles and mortality in critically ill covid-19 patients. Journal of Clinical Microbiology **59**(12), 01229–21 (2021) https://journals.asm.org/doi/pdf/10.1128/JCM.01229-21. https://doi.org/10.1128/JCM.01229-21

[6] Oremland, M., Michels, K., Bettina, A., Lawrence, C., Mehrad, B., Laubenbacher, R.: A computational model of invasive aspergillosis in the lung and the role of iron. BMC Systems Biology **10** (2016). https://doi.org/10.1186/s12918-016-0275-2

[7] Ribeiro, H.A.L., Vieira, L.S., Scindia, Y., Adhikari, B., Wheeler, M., Knapp, A., Schroeder, W., Mehrad, B., Laubenbacher, R.: Multi-scale mechanistic modelling of the host defence in invasive aspergillosis reveals leucocyte activation and iron acquisition as drivers of infection outcome. Journal of The Royal Society Interface **19**(189), 20210806 (2022) https://royalsocietypublishing.org/doi/pdf/10.1098/rsif.2021.0806. https://doi.org/10.1098/rsif.2021.0806

[8] Gong, D., Farley, K., White, M., Hartshorn, K.L., Benarafa, C., Remold-O'Donnell, E.: Critical Role of SerpinB1 in Regulating Inflammatory Responses in Pulmonary Influenza Infection. The Journal of Infectious

Diseases **204**(4), 592–600 (2011) https://academic.oup.com/jid/article-pdf/204/4/592/18066131/jir352.pdf. https://doi.org/10.1093/infdis/jir352

[9] Irvin, C.G., Bates, J.: Measuring the lung function in the mouse: the challenge of size. Respiratory research **4**(1) (2003). https://doi.org/10.1186/rr199

[10] Gago, S., Overton, N., Ben Ghazzi, N., Novak-Frazer, L., Read, N., Denning, D., Bowyer, P.: Lung colonization by aspergillus fumigatus is controlled by znf77. Nature Communications **9** (2018). https://doi.org/10.1038/s41467-018-06148-7

[11] Johnson, J.W., Lebreton, J.M.: History and use of relative importance indices in organizational research. Organizational Research Methods **7**(3), 238–257 (2004) https://doi.org/10.1177/1094428104266510. https://doi.org/10.1177/1094428104266510

[12] Mackel, J.J., Steele, C.: Host defense mechanisms against aspergillus fumigatus lung colonization and invasion. Current Opinion in Microbiology **52**, 14–19 (2019). https://doi.org/10.1016/j.mib.2019.04.003. Host Microbe Interactions: Fungi • Host-Microbe Interactions: Parasitology

[13] Grunwell, J., Giacalone, V., Stephenson, S., Margaroli, C., Dobosh, B., Brown, M., Fitzpatrick, A., Tirouvanziam, R.: Neutrophil dysfunction in the airways of children with acute respiratory failure due to lower respiratory tract viral and bacterial coinfections. Scientific Reports **9**, 2874 (2019). https://doi.org/10.1038/s41598-019-39726-w

[14] Verweij, P., Gangneux, J., Bassetti, M., Brüggemann, R., Cornely, O., Koehler, P., Lass-Florl, C., van de Veerdonk, F., Chakrabarti, A., Hoenigl, M. Lancet Microbe. **1**(2), 53–55 (2020). https://doi.org/10.1016/S2666-5247(20)30027-6.

[15] Arastehfar, A., Carvalho, A., van de Veerdonk, F.L., Jenks, J.D., Koehler, P., Krause, R., Cornely, O.A., S. Perlin, D., Lass-Flörl, C., Hoenigl, M.: Covid-19 associated pulmonary aspergillosis (capa)—from immunology to treatment. Journal of Fungi **6**(2) (2020). https://doi.org/10.3390/jof6020091

[16] Segrelles-Calvo, G., Araújo, G.R.S., Llopis-Pastor, E., Carrillo, J., Hernández-Hernández, M., Rey, L., Rodríguez Melean, N., Escribano, I., Antón, E., Zamarro, C., García-Salmones, M., Frases, S.: Prevalence of opportunistic invasive aspergillosis in covid-19 patients with severe pneumonia. Mycoses **64**(2), 144–151 (2021) https://onlinelibrary.wiley.com/doi/pdf/10.1111/myc.13219. https://doi.org/10.1111/myc.13219

[17] Escobar, N., Ordonez, S.R., Wösten, H.A.B., Haas, P.-J.A., de Cock, H., Haagsman, H.P.: Hide, keep quiet, and keep low: Properties that make aspergillus fumigatus a successful lung pathogen. Frontiers in Microbiology **7** (2016). https://doi.org/10.3389/fmicb.2016.00438

[18] Rodrigues, A.G., Araujo, R., Pina-Vaz, C.: Human albumin promotes germination, hyphal growth and antifungal resistance by Aspergillus fumigatus. Medical Mycology **43**(8), 711–717 (2005) https://academic.oup.com/mmy/article-pdf/43/8/711/2788210/43-8-711.pdf. https://doi.org/10.1080/13693780500129814

[19] Stites, S., Nelson, M., Wesselius, L.: Transferrin concentrations in serum and lower respiratory tract fluid of mechanically ventilated patients with copd or ards. Diseases of the chest **107**(6), 1681–1685 (1995). https://doi.org/10.1378/chest.107.6.1681. Funding Information: Supported by the Department of Veteran Affairs Research Service.